

Activation of METTL3 promotes white adipose tissue beiging and combats obesity
METTL3 in white adipose tissue beiging

Renxiang Xie^{1,2,#}, Sujun Yan^{1,3,#}, Xiaoling Zhou^{1,#}, Yunyi Gao¹, Yu Qian¹, Jingyu Hou¹,
Zhanghui Chen⁴, Kairan Lai⁵, Xiangwei Gao^{1,3,*}, Saisai Wei^{1,2,*}.

1, Sir Run-Run Shaw Hospital, School of Public Health, Zhejiang University School of
Medicine, Hangzhou 310058, China.

2, Key Laboratory of Laparoscopic Technology of Zhejiang Province, Department of
General Surgery, Sir Run-Run Shaw Hospital, Zhejiang University School of Medicine,
Hangzhou 310016, China.

3, Department of Clinical Laboratory, Sir Run Run Shaw Hospital, Zhejiang University
School of Medicine, Hangzhou 310016, China.

4, Zhanjiang Institute of Clinical Medicine, Zhanjiang Central Hospital, Guangdong
Medical University, Zhanjiang 524045, China.

5, Eye Center, Second Affiliated Hospital, Zhejiang University School of Medicine,
Hangzhou 310009, China.

These authors contributed equally.

* Correspondence: Xiangwei Gao, T: +86-57188208169, xiangweigao@zju.edu.cn; or
Saisai Wei, saisaiwei@zju.edu.cn.

SUPPLEMENTARY FIGURE 1

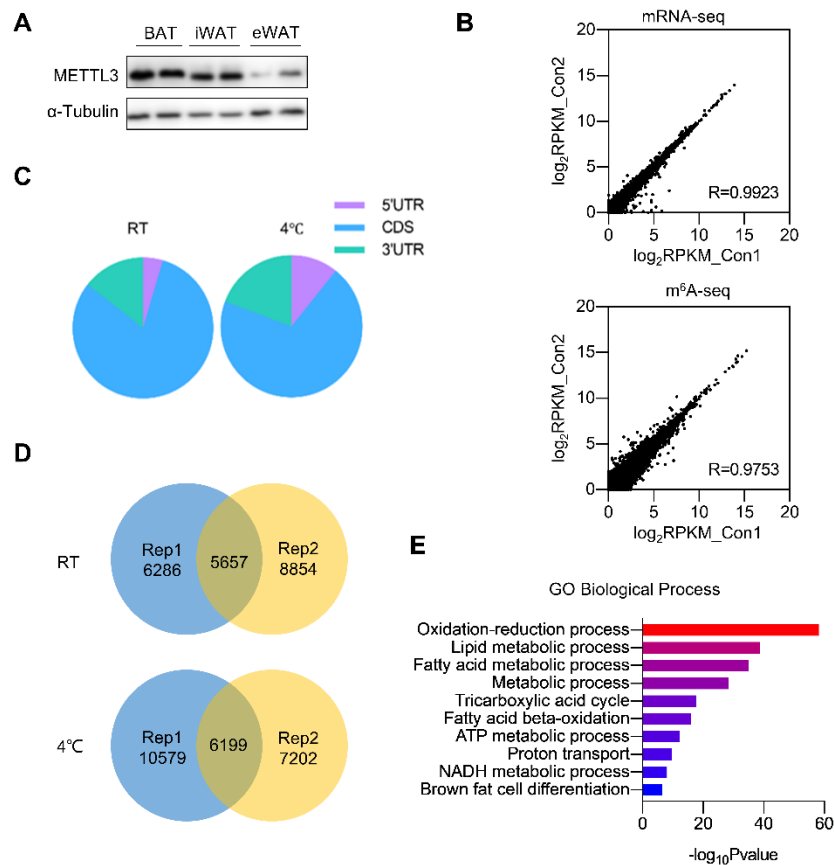
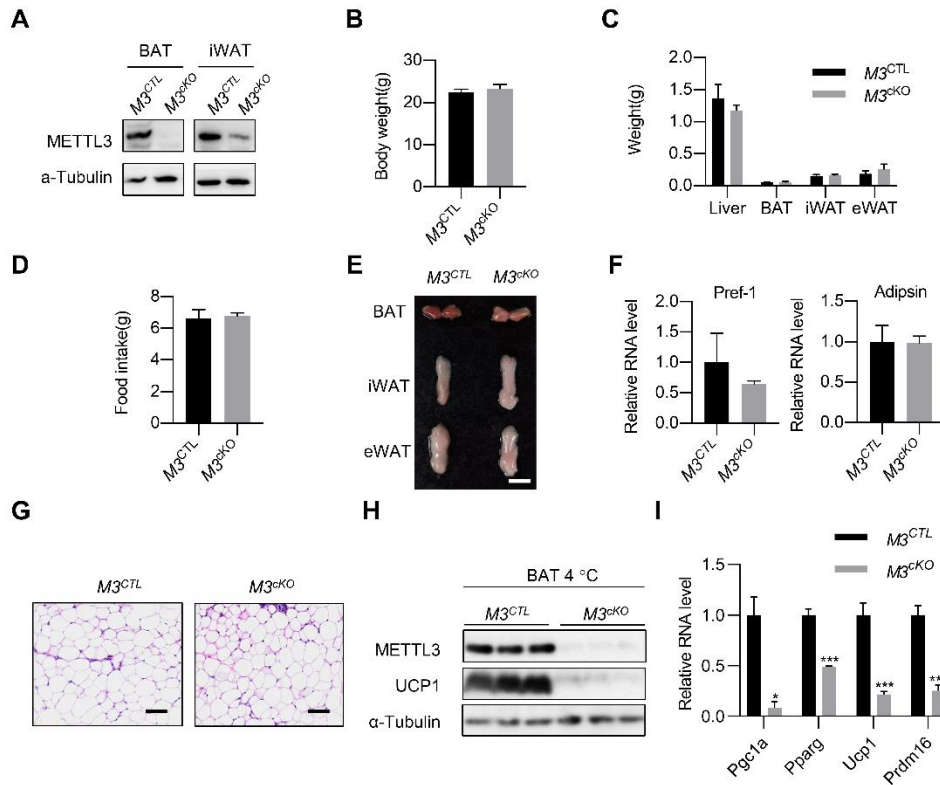


Figure S1. m⁶A profiling of white and beige adipose tissue

(A) Western blot analysis of METTL3 expression in BAT, iWAT and eWAT from mice housed at room temperature. (B) Pearson's correlation of RNA-seq and m⁶A-seq data between two independent replicates of iWAT from mice housed at room temperature. (C) Pie chart showing the proportion of m⁶A peaks among different regions of transcripts in iWAT from mice housed at room temperature or 4 °C (two biological replicates). (D) Venn diagram showing the overlap of m⁶A sites detected from two independent replicates of iWAT from mice housed at room temperature or 4 °C. (E) Top GO terms (biological process) enriched on transcripts with up-regulated m⁶A modification during beiging.

34 **SUPPLEMENTARY FIGURE 2**



35

36 **Figure S2. METTL3 is largely dispensable for WAT adipogenesis**

37 (A) Immunoblot analysis of METTL3 expression in BAT and iWAT from $M3^{CTL}$ and $M3^{cKO}$
38 mice. (B) Bodyweight of $M3^{CTL}$ and $M3^{cKO}$ mice at the age of eight weeks (6 mice in each
39 group, t-test, two-tailed). (C) Weight of liver, BAT, iWAT and eWAT from $M3^{CTL}$ and $M3^{cKO}$
40 mice at the age of eight weeks (6 $M3^{CTL}$ mice, 3 $M3^{cKO}$ mice, t-test, two-tailed). (D) Daily
41 food intake of $M3^{CTL}$ and $M3^{cKO}$ mice at the age of eight weeks (6 mice in each group, t-
42 test, two-tailed). (E) Gross view of BAT, iWAT and eWAT from $M3^{CTL}$ and $M3^{cKO}$ mice. (F)
43 The mRNA levels of *Pref-1* and *Adipsin* in iWAT from $M3^{CTL}$ and $M3^{cKO}$ mice (3
44 independent experiments, t-test, two-tailed). (G) H&E staining of iWAT from $M3^{CTL}$ and
45 $M3^{cKO}$ mice. Scale bar, 50 μ m. (H) Immunoblot analysis of METTL3 and UCP1 expression
46 in BAT of $M3^{CTL}$ and $M3^{cKO}$ mice housed at 4°C. (I) The mRNA levels of thermogenic
47 genes (*Pparg1a*, *Pparg*, *Ucp1*, *Prdm16*) in BAT of $M3^{CTL}$ and $M3^{cKO}$ mice after cold

48 treatment (*P<0.05, ***P<0.001; 3 independent experiments, t-test, two-tailed).

49

50 **SUPPLEMENTARY FIGURE 3**

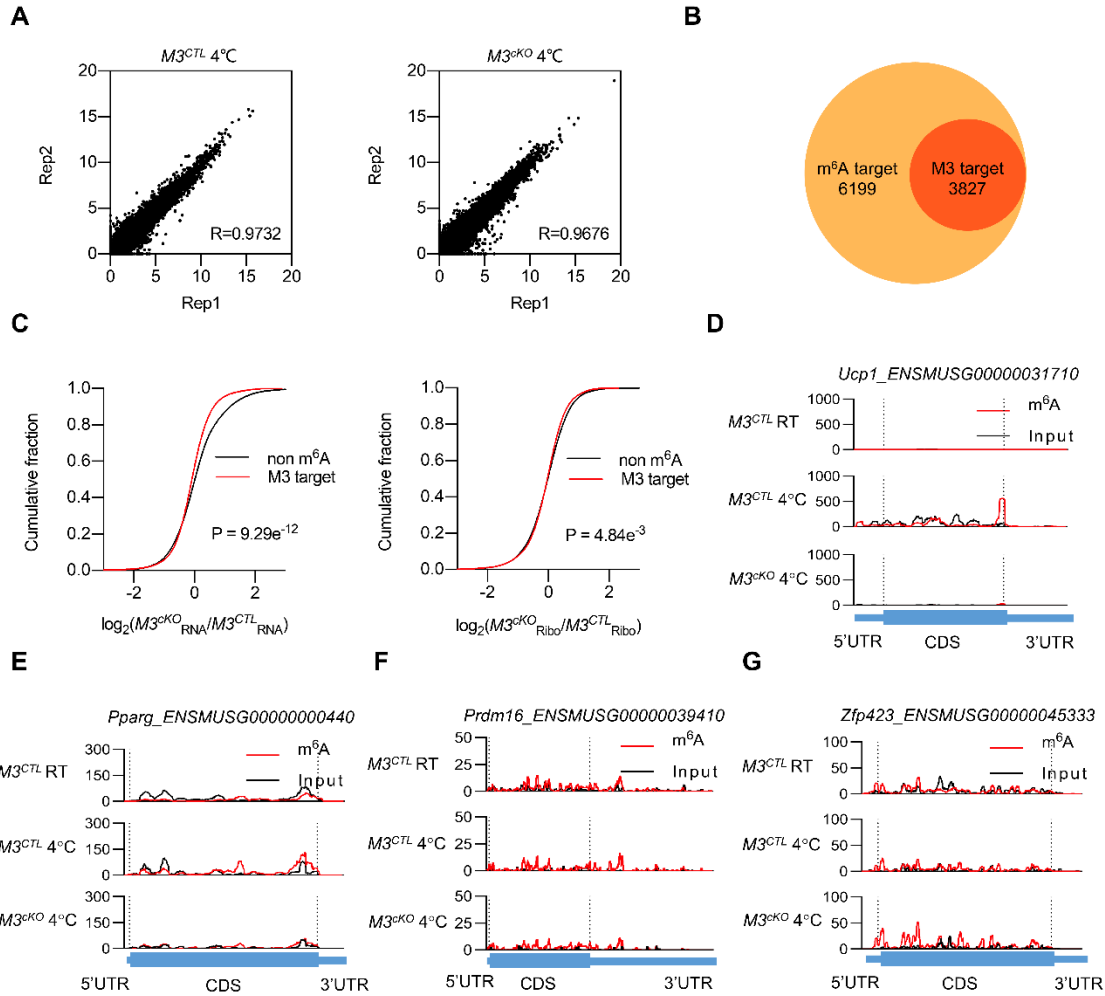


Figure S3. Characteristics of METTL3-targeted mRNA

(A) Pearson's correlation coefficients of Ribo-seq data between two independent replicates in iWAT from *M3^{CTL}* and *M3^{cKO}* mice housed at 4 °C. (B) Venn diagram showing the overlap of *m⁶A* sites and METTL3-targeted *m⁶A* sites. (C) Cumulative distributions showing the alternation of METTL3-targeted and non-*m⁶A* transcripts at mRNA level and translational level between iWAT depots of cold-exposed *M3^{CTL}* and

58 $M3^{cKO}$ mice. Mann-Whitney test. (D-G) The m⁶A distribution within *Ucp1* (D), *Pparg*
59 (E), *Prdm16* (F), and *Zfp423* (G) transcript (two biological replicates).